



## Vertical axis wind turbine – A review of various configurations and design techniques

Muhammad Mahmood Aslam Bhutta<sup>\*</sup>, Nasir Hayat, Ahmed Uzair Farooq, Zain Ali, Sh. Rehan Jamil, Zahid Hussain

Department of Mechanical Engineering, University of Engineering and Technology Lahore, G.T. Road, Lahore, Punjab 54890, Pakistan

### ARTICLE INFO

#### Article history:

Received 5 March 2011

Received in revised form

10 December 2011

Accepted 18 December 2011

Available online 17 February 2012

#### Keywords:

Vertical axis wind turbine analysis

techniques

VAWT

### ABSTRACT

Increased concern for environment has led to the search for more environment friendly sources of energy. Wind energy can be a viable option in this regard. Vertical axis wind turbines offer promising solution for areas away from the integrated grid systems. However, they have certain drawbacks associated with different configurations. This paper reviews various configurations of VAWT along with their merits and demerits. Moreover, design techniques employed for VAWT design have also been reviewed along with their results. It was learned that coefficient of power ( $C_p$ ) for various configurations is different and can be optimized with reference to Tip Speed Ratio. Latest emerging design techniques can be helpful in this optimization. Furthermore, flow field around the blade can also be investigated with the help of these design techniques for safe operation.

© 2011 Elsevier Ltd. All rights reserved.

### Contents

1. Introduction.....	1927
2. Configurations.....	1928
2.1. Darrieus type wind turbine .....	1928
2.1.1. Egg-beater type Darrieus wind turbine .....	1928
2.1.2. Giromill (straight bladed type Darrieus wind) turbine .....	1931
2.1.3. Variable geometry oval trajectory (VGOT) Darrieus turbine.....	1933
2.1.4. Darrieus–Masgrows (two-tier) rotor.....	1933
2.1.5. Twisted three bladed Darrieus rotor .....	1933
2.1.6. Crossflex wind turbine .....	1933
2.2. Savonius rotor .....	1933
2.3. Combined Savonius and Darrieus rotor .....	1934
2.4. Two leaf semi rotary VAWT .....	1934
2.5. Sistan type wind mill.....	1934
2.6. Zephyr turbine .....	1934
3. Design techniques of vertical axis wind turbine .....	1934
3.1. Efficiency .....	1934
3.1.1. Analogy between a flapping wing and Darrieus rotor .....	1934
3.1.2. Impulsive method .....	1935
3.1.3. Buckingham Pi theorem .....	1935
3.1.4. Exergy analysis .....	1936
3.1.5. Computational fluid dynamics (CFD).....	1936
3.2. Aerodynamic load calculations.....	1936

**Abbreviations:** VAWT, vertical axis wind turbine; HAWT, horizontal axis wind turbine; TSR, tip speed ratio; PIV, particle image velocimetry; BEM, blade element momentum; OMA, operational modal analysis; GHE, green house emission; NEXt, natural excitation technique; CFD, computational fluid dynamics; URANS, unsteady Reynolds-averaged Navier–Stokes; SST, shear stress transport; LES, large eddy simulation; DES, detached eddy simulation; VGOT, variable geometry oval trajectory.

<sup>\*</sup> Corresponding author. Tel.: +92 3424112092.

E-mail address: [drbhutta@uet.edu.pk](mailto:drbhutta@uet.edu.pk) (M.M. Aslam).

3.2.1.	Blade element method .....	1936
3.2.2.	Actuator disc method .....	1936
3.2.3.	Dynamic analysis .....	1937
3.2.4.	Impulsive methods .....	1937
3.2.5.	Vortex methods .....	1937
3.3.	Flow field visualization and analysis .....	1937
3.3.1.	Particle image velocimetry .....	1937
3.3.2.	Computational fluid dynamics (CFD) .....	1937
3.4.	Vibration and fatigue calculation .....	1937
3.4.1.	Operational modal analysis .....	1937
3.5.	Analysis of an attachment on blade .....	1938
3.5.1.	Wind tunnel testing .....	1938
4.	Conclusion .....	1938
	References .....	1938

## Nomenclature

$C_p$	coefficient of power = $P_o / \rho A V^3$
$N$	number of blades
$B$	blade thickness
$D$	rotor diameter
$XYZ$	subscript for stationary axes
$xyz$	subscript for rotating axes
$M$	torque
$V_\infty$	free stream velocity
$a, b$	constants
$c$	scaling factor (dimensionless)
$W_o$	work rate
$E$	power
$A$	cross-sectional area
$\psi$	exergy energy
$Ex_f$	wind flow energy
$Ex_p$	physical energy
$Ex_k$	kinematic energy
$\dot{m}$	mass flow rate
$C$	specific heat coefficient
$T$	temperature
$R$	general gas constant
$P$	pressure
$F_T$	thrust force
$d$	axial interference factor
$F$	Prandtl's tip loss correction
$f_g$	Glauert correction
$F_D$	turbine drag force
$F_L$	turbine lift force
$V$	wind velocity
$V_o$	undisturbed wind velocity
$V_a$	induced velocity
$V_w$	wake velocity
$\tau$	stress induced
$K$	kinematic viscosity
$U$	velocity on boundary layer
$\delta$	boundary layer thickness
$H_A$	angular momentum
$I$	inertia of the blade
$\omega$	angular velocity
$\Omega$	operational frequency
$\rho$	fluid density
$\lambda$	tip speed ratio
$\sigma$	constant = 0.28
$\eta$	efficiency

## 1. Introduction

The focus on Renewable Energy Resources has increased significantly in the recent years in the wake of growing environmental pollution, rising energy demand and depleting fossil fuel resources. Different sources of renewable energy include biomass, solar, geothermal, hydroelectric, and wind. Among these resources wind has proved to be a cheaper alternative energy resource and hence extensive research efforts have been put to improve the technology of electricity generation through wind. The world has enormous potential of wind energy that can be utilized for electricity generation. Fig. 1 shows the wind velocities at various locations around the world. In areas where favorable sites exist, it has already been preferred over conventional fossil fuels for electricity generation [1]. Wind power is now the world's fastest growing energy resource [2]. Fig. 2 shows that installed wind generation capacity has increased from 25,000 MW to more than 200,000 MW in 10 years (from 2001 to 2010). Although the vertical axis wind turbine (VAWT) was the first ever wind turbine to be used for harnessing wind energy, researchers of the modern era lost interest in it due to the initial perception that VAWT cannot be used for large scale electricity generation. Horizontal axis wind turbine (HAWT) remained the focus of all wind energy related research activity for last few decades. That is why major portion of the installed capacity shown in Fig. 2 comprises of HAWTs.

However, research work on VAWT continued in parallel at a relatively smaller scale. Scientists and Engineers developed various wind turbine configurations and utilized different approaches for their analysis. Optimum conditions for the working of VAWTs were determined. The details of these techniques and configurations along with the major findings of researchers on vertical axis wind turbines are reviewed in this paper. A closer look on the concepts leads towards the fact that VAWTs are suitable for electricity generation in the conditions where traditional HAWTs are unable to give reasonable efficiencies such as high wind velocities and turbulent wind flows. Another major advantage is that VAWTs are omni-directional, accepting wind from any direction without any yawing mechanism [3]. A comparison between VAWTs and HAWTs is made in Table 1. It is evident from the table that VAWT has a number of promising features which if exploited properly can make it a better alternative.

Solutions to the inherent problems of VAWTs such as "Blade lift forces" and "Blade fatigue caused by varying loads due to turbulent flow" are presented but more research input is required [4,5]. Currently, large scale VAWTs are not economically attractive; however, they offer energy solutions for remote places away from the main distribution lines and places where large wind farms cannot be installed due to environmental concerns and small scale dispersed generation units are preferred [6]. That is why mass

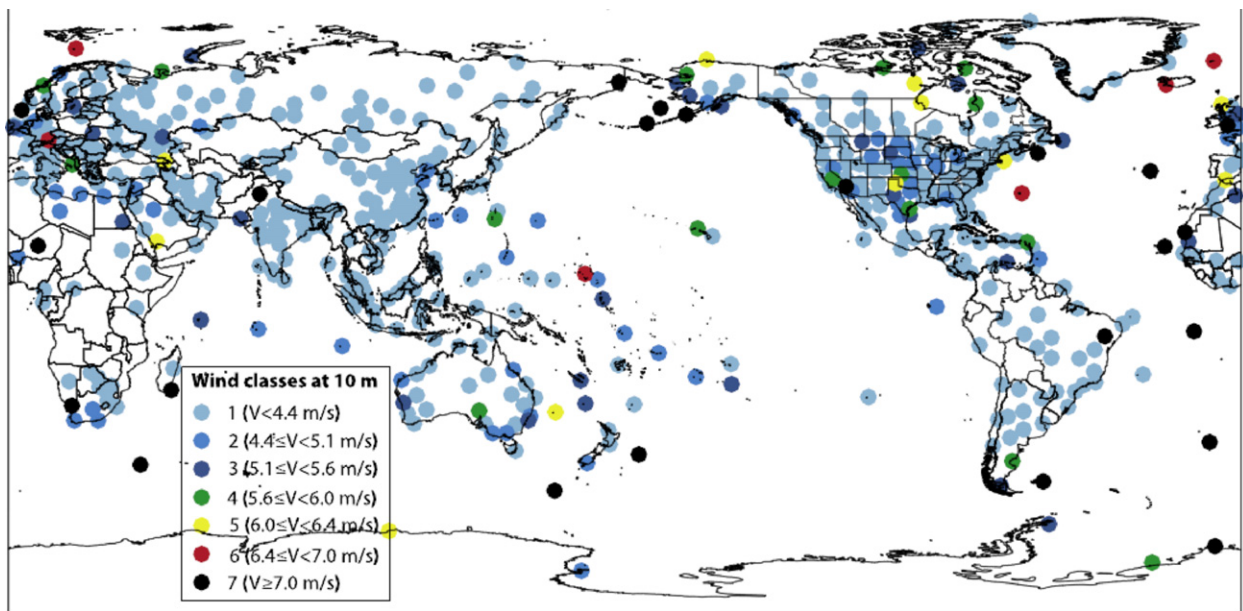


**Fig. 1.** Average wind velocity in different regions of the world [1].

production of VAWTs has recently been started as small scale wind power generating units [7].

## 2. Configurations

A great degree of design versatility exists in the vertical axis wind turbines as shown in Table 2. There are a few problems inherent to the currently available designs including low starting torque, blade lift forces, low efficiency, poor building integration, etc. In the past few decades, the engineers came up with many new and innovative design approaches to resolve these issues associated with VAWTs. A detailed review of VAWT configurations available till now and the work done on each configuration has been discussed in the following sections.

### 2.1. Darrieus type wind turbine

Darrieus wind turbine designs were first patented in 1931. These types of turbines have highest values of efficiency among VAWTs but generally suffer from problems of low starting torque and poor building integration. Darrieus type wind turbines have many variants, as discussed in the following lines, all of which are Lift-type

**Table 1**  
Merits of vertical axis wind turbines over horizontal axis wind turbines.

	Vertical axis wind turbine (VAWT)	Horizontal axis wind turbine (HAWT)
Tower sway	Small	Large
Yaw mechanism	No	Yes
Self starting	No	Yes
Overall formation	Simple	Complex
Generator location	On ground	Not on ground
Height from ground	Small	Large
Blade's operation space	Small	Large
Noise produced	Less	Relatively high
Wind direction	Independent	Dependent
Obstruction for birds	Less	High
Ideal efficiency	More than 70%	50–60%

wind turbines, i.e. lift forces acting on the blades of turbine cause the rotor to rotate and hence generate electricity.

#### 2.1.1. Egg-beater type Darrieus wind turbine

It contains two or more blades arranged as arms of an egg-beater as shown in Table 2. The mechanism of torque generation in this type of Darrieus wind turbine is different from that of a horizontal axis wind turbine. The flow around the blades of a Darrieus wind turbine is essentially unsteady. This pulsating flow produces a thrust force which is proportional to the geometry of blade and the amplitude and frequency of the pulsating flow [8,9].

The complex egg-beater type geometry provides for minimum bending stresses in the blades [10]. Due to this enhanced mechanical integrity and high co-efficient of performance commercial Turbines as large as capacities of 3.8 MW have been produced in Canada [11]. Marini et al. [12] performed the aerodynamic analysis of Darrieus turbine models and plotted  $C_p$  against the velocity of approaching wind. The highest values thus obtained were 0.42

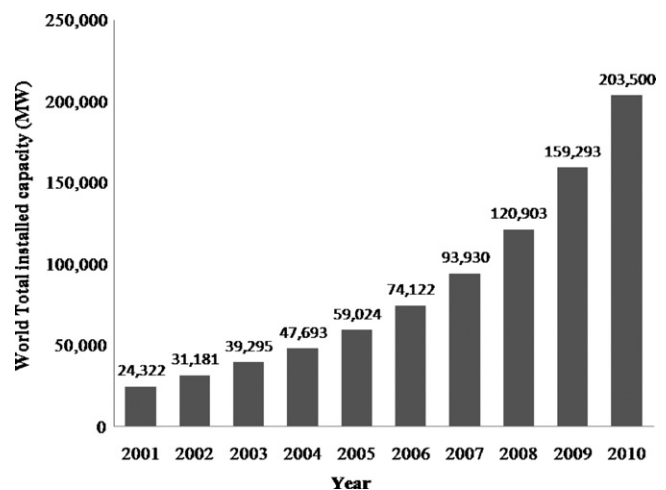


**Fig. 2.** Installed wind potential of the world [World Wind Energy Association].

**Table 2**  
Summary of wind turbine configurations.

Sr. no.	Wind turbine type	Figures	Max. capacity available	Features	Merits	Demerits
1.	Darrieus rotor – egg beater shaped Islam et al. [10]	Fig. 3 [51]	4 MW	> Lift type wind turbine  > Curved blades with varying cross-section	> Suitable for high power applications	> Complicated shape  > High cost
2.	Gorelov and Krivospitsky [9] Eriksson et al. [11] Brahimi and Paraschivoiu [14] Rosen and Abramovich [15] Bergeles et al. [16] Marini et al. [12] Wakui et al. [17] Staelens et al. [20] Shienbein and Malcolm [13] Darrieus rotor – straight bladed Islam et al. [10]	Fig. 4 [52]	10 kW	> Lift type wind turbine  > Aerofoil shaped blades with constant cross-section	> Simple in construction  > Low cost	> Low starting torque  > Low power coefficient in laminar flow as compared to HAWT
3.	Gorelov and Krivospitsky [9] Eriksson et al. [11] Vandenberghe and Dick [22] Graham et al. [24] Takao et al. [25] Wilhelm et al. [26] Siota et al. [21] Howell et al. [18] Darrieus rotor – VGOT  Ponta et al. [2]		Prototype only	> Lift type wind turbine  > Unique design > No central axis  > Blades instead of rotating in atmosphere, slide over rails and rotary motion of wheels generate electricity	> Increased swept area results in high rated power without decrease in rotational speed	> Expensive  > Complicated design > Only feasible for high power applications
4.	Darrieus–Masgrowe	Fig. 5	3 kW	> Lift type wind turbine	> Self starting capability	> Designed and tested only for low power applications
5.	Gorelov and Krivospitsky [9] Twisted three bladed Darrieus rotor Gupta and Biswas [27]		Prototype only	> Typical straight bladed Darrieus rotor is divided into two tiers shifted by 90° > Lift type wind turbine  > Aerofoil shape twisted by 30° at trailing edge	> Decrease in flow separation results in better aerodynamic performance	> Intricate aerofoil shape  > Low power coefficient

6.	Crossflex Sharpe and Proven [28]	Fig. 6	Prototype only	> Lift type wind turbine	> Good building integration	> Only suitable in high rise buildings
7.	Savonius rotor Islam et al. [10]	Fig. 7	4.5 kW	> Multiple Darrieus rotors on a single frame > Drag type wind turbine > Half-cylinder discs attached to the central rotor	> Good efficiency > Good starting torque	> Low efficiency
8.	Gorelov and Krivospitsky [9] Mohamed et al. [29] Combined Savonius and Darrieus rotor Wakui et al. [17]	Fig. 8	Prototype only	> Lift-drag type wind turbine  > Darrieus rotor combined with Savonius rotor on the same shaft	> Good starting torque and efficiency	> Complex design
9.	Debnath et al. [30]. Gavalda et al. [31] Two leaf semi rotary Zhang et al. [32]	Fig. 9	Prototype only	> Drag type wind turbine  > Two flat plates, oriented at different angles, attached to a central rotating shaft	> High power coefficient > Self start ability	> Not suitable for high power
10.	Sistan wind mill Al-Hassan and Hill [33] Muller et al. [34]	Fig. 10	1.8 kW	> Drag type wind turbine Straight bladed drag type	> Simple structure > Good building integration	> Poor efficiency
11.	Zephyr turbine Pope et al. [35]	Fig. 11	Prototype only	> Lift type wind turbine  > Guide vane rows around rotor	> Good efficiency	> Complex construction > Occupies large area



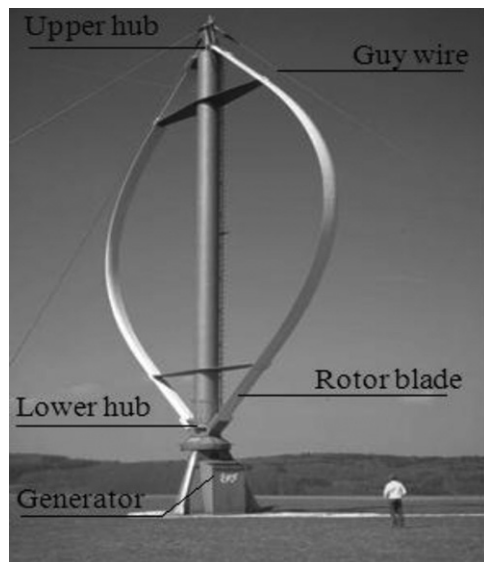


Fig. 3. Darrieus rotor – egg beater shaped wind turbine [51].

at particular TSR. Shienbein and Malcolm [13] studied 50 kW and 500 kW models of Darrieus wind turbines and presented their findings on mechanical and control systems of the turbines as well as their economical and performance analysis.

Although this design is among the first ones to be produced for large scale power generation, the difficulty in manufacturing of complex geometry of blades and the associated high costs have limited its production at commercial scale [11]. Moreover, the design suffers from the issue of low starting torque and is unable to self start at low wind speeds.

Various authors have contributed towards the designing and optimization of this turbine type. Brahimi and Paraschivoiu [14] calculated structural loads on the Darrieus rotor wings in turbulent flow conditions. Rosen and Abramovich [15] also carried out detailed study on the structure of Darrieus rotor blades. They presented a theoretical model which can be used to analyze the behavior of blades under different loading configurations. The theoretical model was also tested experimentally. Bergeles et al. [16] carried out flow field study of Darrieus wind turbine experimentally. The wake effect of the turbine blade rotors was studied in detail. Wakui et al. [17] analyzed the wind turbine generator systems for this type of wind turbine configuration. They concluded

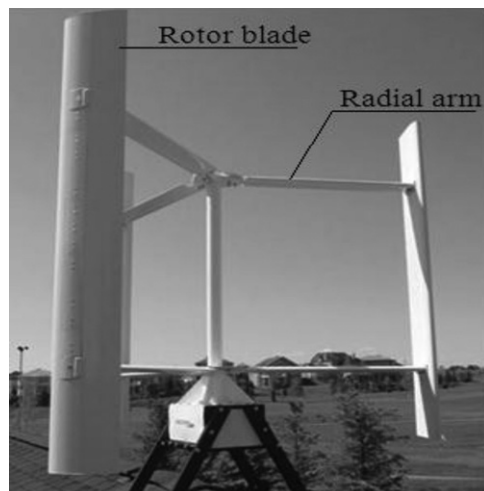


Fig. 4. Darrieus rotor – straight bladed wind turbine [52].

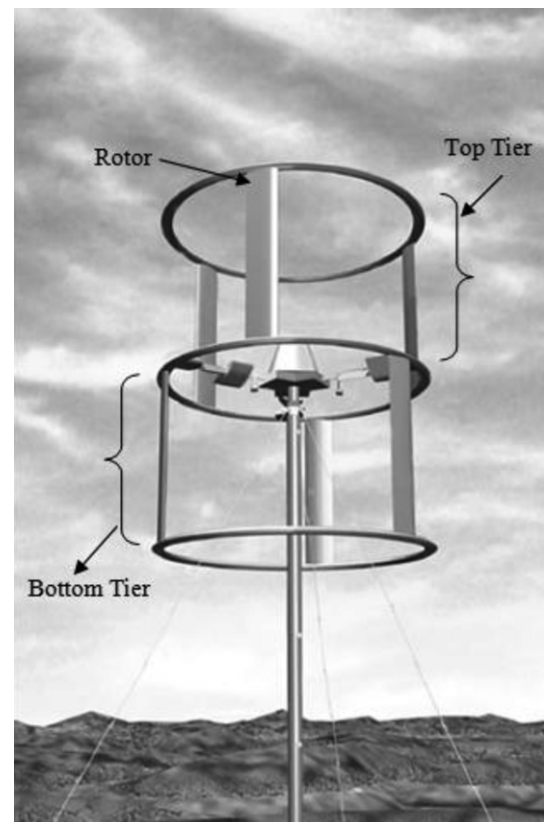


Fig. 5. Darrieus rotor – VGOT wind turbine [9].

that a unique operating system should be designed for optimum power generation in particular wind conditions and for a particular wind turbine configuration.

#### 2.1.2. Giromill (straight bladed type Darrieus wind) turbine

The curved egg-beater type blades are replaced by straight blades having aerofoil cross-section as seen from the top of the turbine to give a new configuration of VAWT known as straight

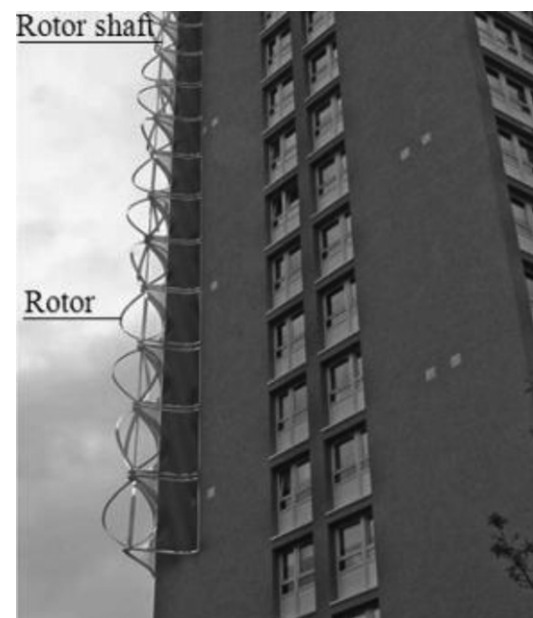


Fig. 6. Crossflex wind turbine [28].

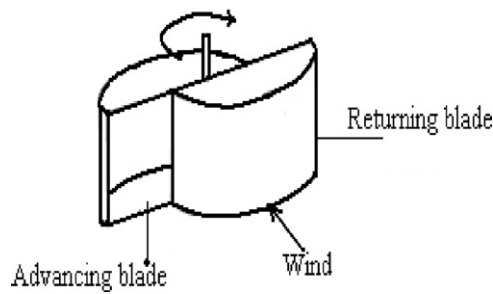


Fig. 7. Savonius rotor [29].

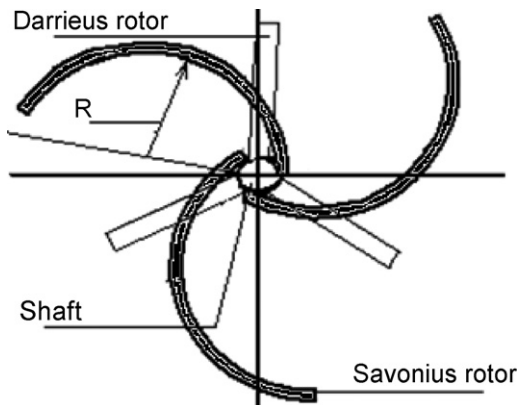


Fig. 8. Combined Savonius and Darrieus rotor [30].

bladed Darrieus type or Giromill as shown in Table 2. It can have any number of blades starting from one to commercially available five bladed configurations. However, commonly occurring configurations are two and three bladed. A two bladed Giromill is frequently referred to as an H-rotor [18,19]. These blades can have fixed or variable pitch [9].

Small scale, fixed pitch, roof top designs are commercially available for domestic and other applications. Apart from having comparatively high values of  $C_p$  (0.23), variable pitch blades have the potential to overcome the starting torque issues associated with VAWTs [10,18]. Moreover, the efficiency of the turbine can

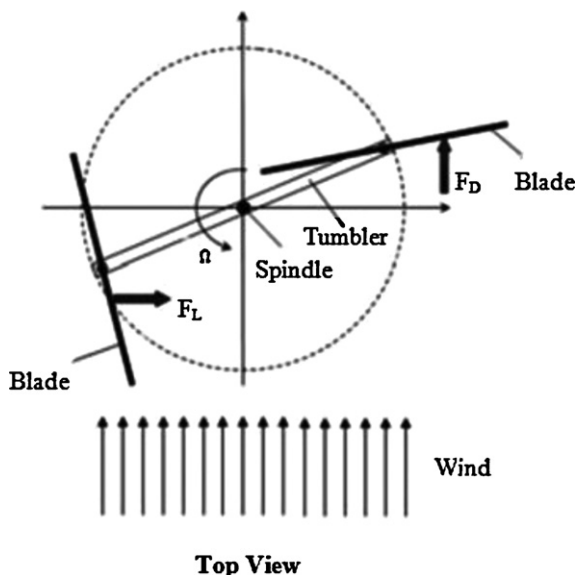


Fig. 9. Two leaf semi rotary VAWT [32].

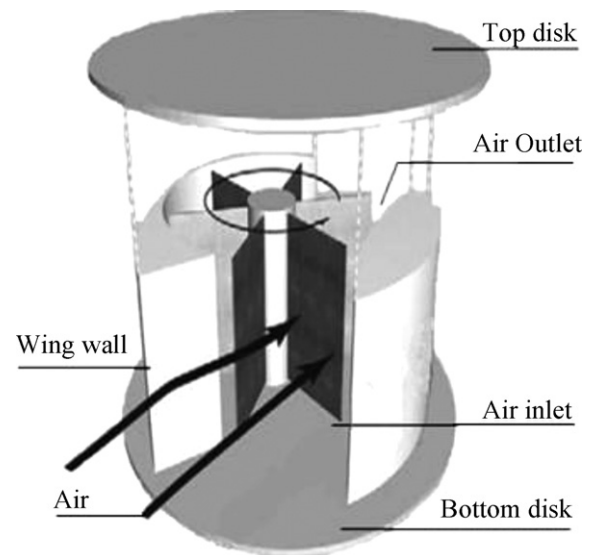


Fig. 10. Sistan wind mill [34].

be further enhanced by varying the angle of attack on the blades in a sinusoidal pattern [20]. Siota et al. [21] worked on electrical systems associated with this type of VAWT. They studied the use of Control Circuit (CC)-Less generation system for this type of turbine and found many advantages over conventional inverter-type and rectification-type generators. They found high level of suitability of CC-Less system for straight bladed VAWT provided the gear box design is modified properly. Relatively lower initial cost is also an added advantage.

Fixed pitch blades, although having a simple construction, give poor starting torque. Variable pitch designs have many advantages over fixed pitch but the construction is very complicated hence reducing the cost-effectiveness of the turbine for small scale applications [10].

Authors contributing to the designing and optimization include Vandenberghe and Dick [22] who carried out a detailed aerodynamic study of this type of configuration. Their results can be used for 'parametric optimization' of the wind turbines. Islam et al. [23] also discussed various aerodynamic effects on this configuration such as dynamic stall and wake effect. Graham et al. [24] presented

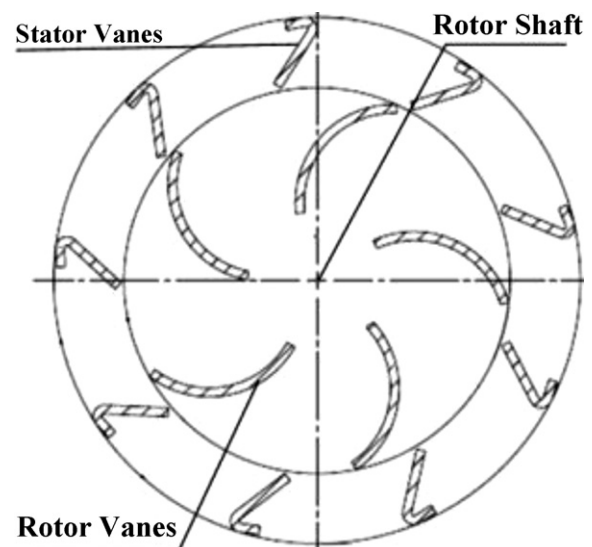


Fig. 11. Zephyr turbine [35].

a selection procedure for aerofoil selection for blades of the rotor. Takao et al. [25] worked on improving the performance parameters by addition of guide vane row around the turbine. As a result they observed an increase in power coefficient to 0.215, which is 1.8 times higher than that of the original turbine without any guide vane row. Wilhelm et al. [26] presented circulation control methods for the performance improvement thereby increasing power coefficient and improving self starting characteristics through 'lift augmentation'. Howell et al. [18] performed aerodynamic analysis by using fluid flow simulations as well as wind tunnel testing. Their results indicate that the coefficient of power ( $C_p$ ) increases till tip speed ratio '2' and afterwards a declining trend is observed.

#### 2.1.3. Variable geometry oval trajectory (VGOT) Darrieus turbine

The earlier designs of Darrieus rotor discussed so far could not be used for very large scale power generation because of the low rotor speed which is an inherent characteristics of the rotor design [2]. Ponta et al. [2] studied large scale applications of Darrieus rotor and presented a new configuration. In this design the blades, instead of revolving around a central rotor, move on rails on an elevated rail track. The wheels attached to the base of blades are coupled with electrical systems to generate electricity.

The new design promises the possibility of large scale power generation through vertical axis wind turbines. It combines the omnidirectional nature of VAWT with high efficiency (as high as 57% at optimum design configurations) and increased structural stability and eliminates the issues of low starting torque [2].

Despite all the predicted benefits, the design has yet to prove its capabilities through a fabricated prototype. Moreover, the complexity of design does not favor its application at small scale, roof top scenario.

Detailed numerical models are, however, developed by Ponta et al. [2] for the analysis of VGOT Darrieus Turbine and three new dimensionless constants namely equivalent power coefficient, equivalent solidity coefficient, and trajectory efficiency were introduced to analyze the performance of this configuration. The values of power coefficient ( $C_p$ ), calculated for different number of blades ' $N$ ', are shown against TSR. The results show that the turbine with higher number of blades ( $N = 120\text{--}160$ ) has good efficiency at low TSR ( $\sim 2$ ) while at higher TSR, comparatively a lesser number of blades ( $N = 60\text{--}80$ ) show better efficiency.

#### 2.1.4. Darrieus–Masgrows (two-tier) rotor

A two-tier configuration for straight bladed Darrieus rotor was suggested by Gorelov and Krivospitsky [9] which is called Darrieus–Masgrows rotor. The turbine assembly is divided into two tiers with two or three blades in each tier. The two-tiers are shifted by an angle of  $90^\circ$ . An erected prototype is shown in Table 2. The new configuration has same mechanism of torque generation as other Darrieus rotors.

The two-tier configuration facilitates the operation by enabling the turbine to self start at wind velocity as low as 1.6–2 m/s with efficiency of 39–40% and thus eliminating the use of variable pitch rotor.

The experiments conducted by Gorelov and Krivospitsky [9] show that the assembly exhibits self-start at a 'sufficiently larger width of blades' which is given by the equation,

$$B = \frac{N \cdot \sigma}{D} \quad (1)$$

where ' $B$ ' is the blade thickness, ' $N$ ' is the number of blades, ' $D$ ' is the rotor diameter and ' $\sigma$ ' is a constant whose value is 0.28 for maximum value of  $C_p$  (0.4 approx.).

Further study is however required on this configuration to prove its feasibility for large scale applications which should also include structural stability of the two-tier rotor as well.

#### 2.1.5. Twisted three bladed Darrieus rotor

Gupta and Biswas [27] worked on the idea of twisted blades of a Darrieus rotor at the trailing edge. Experiments and computational fluid dynamics (CFD) simulations were performed on the new configurations which showed promising results.

One of the main advantages of the twisted blades, as discussed by Gupta and Biswas [27], is that a twisted rotor blade helps reducing flow separation. The resulting rotor thus has a positive lift at zero angle of incidence enabling it to self start at favorable wind conditions (where ordinary Darrieus rotor may require auxiliary mechanism for starting). It can also contribute to increase in efficiency as the 'positive wetted portion' of blade will increase hence increasing the projected area of the blade.

The main drawback of this configuration is the complexity involved in the fabrication of twisted blades that increases with the size of turbine. Moreover, in the work of Gupta and Biswas [27], the  $C_p$  value obtained is very low (0.128). Such low values are unacceptable for commercial applications of the turbine. However, future study can be made with alterations in aerofoil design, angle of twist and unequal radii of rotation for the rotor (as suggested by Gupta and Biswas [27] to improve turbine efficiency).

#### 2.1.6. Crossflex wind turbine

All the configurations of VAWT discussed above share one common drawback. Their use on high rise buildings is limited by the structural design requirements and architectural aesthetics. Sharpe and Proven [28] presented the idea of Crossflex wind turbine as "true building integrated wind turbine". The idea uses the already introduced concept of Darrieus wind turbine but in an innovative configuration. The conventional Darrieus type turbine is installed within a frame and several such units are usually joined together. Crossflex turbine installed on a building is shown in Table 2.

Sharpe and Proven [28] stated that the efficiency of the turbine is improved by introducing "low inertial mass design". Flexibility of the blades used reduces the bending stresses induced in the blades. As the supporting frame structure is stronger, lower vibrations are produced. As the case with other VAWTs, this turbine can also extract energy from all wind directions and in turbulent flow conditions persisting frequently the vicinity of high rise buildings. The ease with which these turbines can be installed at various locations on a building leads to greater installed capacity per building if all the walls and corners, etc. are utilized. Prototypes of this configuration have already been installed at Newberry tower in Glasgow, Scotland.

This configuration, however, has limited or no applications in wind farm arrangements or low rise buildings.

Through experimental study, Sharpe and Proven [28] created a plot between free stream velocity and power generated which shows that at higher free stream velocity, i.e. greater than 14 m/s, there is a sudden rise in the power produced. Hence, the plot suggests that the installation of this type of turbine is suitable only in the areas where free steam velocity is greater than 14 m/s.

#### 2.2. Savonius rotor

Savonius rotor consists of cup-shaped half, hollow cylinders fixed with a central rotating shaft as shown in Table 2. The torque is generated due to the drag force acting on the half cylinders [10].

The flow energy utilization of Savonius rotor (20%) is lower than that of Darrieus rotor [9]. Hence this type of turbine is generally not used for high-power applications and usually used for wind velocimetry applications [10].

The greatest advantage of a Savonius rotor is its ability to self start in contrast to other 'Lift type' VAWTs [29]. If efficient turbine designs are developed, then this configuration can be used successfully at commercial scale for power generation applications.



Mohamed et al. [29] carried out extensive research for the design optimization of Savonius rotor for its utilization as an energy source at commercial scale. They worked on the concept of obstacle plate in a Savonius rotor at optimum configuration to improve the efficiency of the rotor. Maximum value of power co-efficient observed was '0.3'. Moreover, they also optimized the shape of the rotor in the presence of obstacle plate to obtain a 30% rise in the power co-efficient in the entire operating range [29]. The results indicate that up to TSR '0.7', coefficient of power ( $C_p$ ) increases after which there is a decrease which becomes significant at TSR '1.2'. Moreover, results of Realizable  $k-\varepsilon$  model are remarkably in good agreement with the experimental results.

### 2.3. Combined Savonius and Darrieus rotor

Both the Savonius and Darrieus configurations have their merits and demerits. Savonius rotor gives high value of starting torque while Darrieus rotor gives a low value. When considering efficiency, Darrieus rotor takes the lead over Savonius rotor [30].

In order to take advantage of the merits of both the configurations, a combination of the two rotors was suggested by Gavalda et al. [31], Gupta and Biswas [27] and Debnath et al. [30] and is shown in Table 2. It was found that the co-efficient of power can be as high as 0.35 for different overlap percentages [30]. Moreover, a high torque co-efficient was obtained which showed the ability of self start at low wind velocity. Further study is however required to show the validity of these results for large scale commercial applications.

The variation of coefficient of power ( $C_p$ ) with tip speed ratio was plotted by Debnath et al. [30]. It was observed that up to TSR '0.36', coefficient of power increases to 0.33 and afterwards with increase in TSR first there is a decrease and then an increase in the values of coefficient of power is observed.

Wakui et al. [17] studied the generator systems of this type of turbine as well through dynamic simulations and presented their conclusion that a custom system should be designed to suit each turbine configuration and wind flow conditions.

### 2.4. Two leaf semi rotary VAWT

Zhang et al. [32] worked on the idea of two leaf semi-rotary VAWT with two blades at an angle of 90°. The schematic diagram is shown in Table 2.

This configuration gives higher wind energy utilization factor because of the "non-uniform wind movement". Moreover, it has better self-starting capabilities. Features such as simple construction, ease of installation and maintenance make it more suitable for mountain areas and off grid power supply [32]. However, questions related to structural stability of the blades of large sized models and at high wind speeds remain unanswered.

### 2.5. Sistan type wind mill

One of the earliest wind turbines was used in areas of Sistan and Khorasan of modern Iran [33]. The Sistan wind turbine is a drag force driven turbine. Muller et al. [34] have worked on the aerodynamic modeling of these turbines. The 3-D model of this turbine is shown in Table 2.

These turbines are of special interest due to their inherent ease of building integration. Muller et al. [34] have suggested improvements in the traditional turbine designs by adding disks at top and bottom of the rotor which can improve efficiency to as high as 30%. Moreover, it is suggested that an increase in the turbine blades from 4 to 6 can have a further increase in efficiency of 6–7%. As it is a drag type wind turbine, the ability to self start is inherently present. According to Muller et al. [34], simple construction, solid

view and good efficiency make Sistan type wind mill a real building integrated wind turbine. However more research is required in the field to correctly identify the optimum configurations for the turbine.

### 2.6. Zephyr turbine

This turbine uses stator vanes with reversed winglets as shown in Table 2. The flow first enters a ring of stationary stator blades which allow the wind to leave at a particular angle of incidence. The wind then strikes the rotor blades where its power is harnessed.

Use of stator vanes reduces turbulence in flow thereby decreasing aerodynamic loading on turbine blades [35]. It ensures good mechanical integrity of the entire system. The power co-efficient ( $C_p$ ) obtained by Pope et al. [35] is 0.12. Having too low  $C_p$  values, these designs are currently unacceptable for commercial applications. However, further research on the configuration can optimize parameters that include blade design, stator vane design, distance between stator ring and rotor, etc. to improve turbine efficiency.

Pope et al. [35] derived equations which relate the power coefficient ( $C_p$ ) with TSR and their result shows that at TSR '0.4' the maximum value of  $C_p$  is obtained while it decreases afterwards with increase in TSR. The results can be utilized for further work on this configuration.

## 3. Design techniques of vertical axis wind turbine

Prediction of aerodynamic performance of the wind turbines discussed in the previous section is crucial to their design optimization. Different parameters such as power and torque coefficients, and aerodynamic loads need to be determined and flow field around the rotor has to be visualized in order to carry out the performance analysis. Over the last two decades, there has been significant development of analytical, computational and experimental techniques for fluid flow analysis around an aerofoil in general and vertical axis wind turbine in particular. In the following lines we shall discuss the different techniques utilized by researchers and the aerodynamic characteristics that were determined using these techniques (Table 3).

### 3.1. Efficiency

Efficiency is one of the most important parameters to analyze the performance of a wind turbine design. Efficiency of a wind turbine is expressed usually in terms of flow energy utilization factor and coefficient of power ( $C_p$ ). Recently exergy efficiency (or 2nd law efficiency) has also been employed to analyze the performance of VAWT. These different approaches and relevant techniques are briefly discussed in the following lines.

#### 3.1.1. Analogy between a flapping wing and Darrieus rotor

Gorelov [8] presented a new approach to the efficiency calculation of a Darrieus type vertical axis wind turbine in contrast to conventional approach of lift and drag as in the case of HAWT. They suggested that the mechanism of torque generation in Darrieus rotor is essentially different and resembles closely to the flapping wing of a bird. A pulsating flow of air occurs around the Darrieus rotor which causes a thrust to act on the rotor blades giving the rotor a rotational acceleration about its central axis.

The maximum value of efficiency for a HAWT is limited by Betz's law to be at 59.3%. Based on this newly introduced model by Gorelov [8], an experiment was performed for an 'ideal' Darrieus rotor. The 'ideal' rotor was made of two discs having rotor blades attached in between. The effect of connecting arms of rotor and shaft was, hence, avoided. The efficiency was calculated using the following

**Table 3**

Design techniques of vertical axis wind turbine.

Techniques	Authors	Results
Efficiency Analogy between a flapping wing and Darrieus rotor	Gorelov [8]	> Thrust force generates torque in VAWT unlike lift force in HAWT  > Based on above postulate, maximum efficiency for an ideal Darrieus rotor increased to 72% which was 59.3% according to Betz's law
Impulsive method	Kopeika and Tereshchenko [36]	> This method can be employed for the calculation of power coefficient, drag coefficient and lift coefficient of VAWT on the same pattern as that of HAWT
Buckingham Pi theorem	Pope et al. [37]	> Development of a new correlation which can directly calculate coefficient of power for given TSR
Exergy analysis	Pope et al. [38]	> Exergy analysis can categorically identify the areas for improvement in efficiency of a turbine > Through the analysis, it is clear that there is a room for improvement of VAWT as compared to HAWT
CFD	Debnath et al. [18]	> CFD can successfully be employed for the calculation of power coefficient. A good agreement of results exists between computational and experimental values if correct prediction of fluid flow model can be made
	Howell et al. [25] Mohamed et al. [29]	
Aerodynamic load calculations Blade element method	Hansen et al. [39]	> Aerodynamic loads can be calculated by using this method > It is simple and provides reasonable accuracy > It is more accurate but relatively complex than blade element method
Actuator disc method	Hansen et al. [39]	> Apart from aerodynamic loads, it also estimated blade vibratory stresses with good accuracy
Dynamic analysis	Biswas et al. [40]	> It can perform aerodynamic calculations but cannot be used for calculations of overloaded rotor
Impulsive methods	Kopeika and Tereshchenko [36]	These methods can be used to determine:
Vortex methods	Kopeika and Tereshchenko [36]	> Aerodynamic load calculations > Aerodynamic coefficients > Efficiency of turbine
Flow field visualization and analysis Particle image velocimetry CFD	Fujisawa and Takeuchi [43] Wang et al. [46] Ferreira et al. [47]	> Dynamic stall phenomenon is prominent at low tip speed ratios ( $\lambda = 1, 2, 3$ ) in case of a VAWT > CFD can also be employed for flow visualization Various models of CFD can be employed for the purpose, some conclusive results are: > Out of the two URANS models, SST $k-\omega$ model is better than standard $k-\omega$ model > Large eddy models are more advanced than URANS models > Out of the two large eddy models, DES being combination of LES and URANS models is better and cheap option than LES model
Vibration and fatigue calculation Operational modal analysis	Carne and James [48]	> It can determine both structural and aero-elastic, total system damping of an operating wind turbine > it can also predict modal frequencies for different rotational speeds of wind turbine > It can be used for both horizontal and vertical axis wind turbines
Analysis of an attachment on blade Wind tunnel testing	Li et al. [50]	> Attachment on blade reduces power coefficient proportional to wind speed and mass of attachment

equation relating efficiency with the Torque 'M', free stream velocity 'V<sub>∞</sub>' and angular velocity of shaft 'ω',

$$\eta = \frac{2M\omega}{\rho V_{\infty}^3 A} \quad (2)$$

The flow energy utilization for Darrieus rotors comes out to be 72% from the above mentioned equation. However, the value of efficiency is much lower (~23%) in case of an actual Darrieus rotor due to the effect of connecting arms on the flow field [8].

### 3.1.2. Impulsive method

The aerodynamic coefficients, i.e. the lift coefficient, the drag coefficient and the power coefficient can be estimated by calculating the impulse loss of the flow going through the area swept by the rotor and the averaged-in-time of total aerodynamic force which is applied to the blades [36].

### 3.1.3. Buckingham Pi theorem

In 2010, Pope et al. [37] presented a new model which could predict the performance of drag type VAWT. They developed a power correlation using Buckingham-Pi theorem for vertical axis wind

turbine and tested it on Zephyr type VAWT. The relation developed between coefficient of power ( $C_p$ ) and tip speed ratio (TSR) is given below.

$$C_p = a(\text{TSR})^2 + b(\text{TSR}) + c \quad (3)$$

They also determined experimentally, the values of constants for different configurations of a Zephyr wind turbine by Pope et al. [35]. The equations indicate a nonlinear rise of  $C_p$  with rise in TSR. The model predicted power coefficient with changes in rotor length, stator angle, tip speed ratio (TSR), and stator spacing, to within 4.4% of numerical calculation. Additionally, it was capable of predicting power coefficient with changes in stator spacing, stator angle, and rotor length, to within 3% of numerical results. With correct measurement of the constants, the correlation developed by authors provides useful tool for analysis and improvement of Drag type vertical axis wind turbines [37].

### 3.1.4. Exergy analysis

In 2010, Pope et al. [38] evaluated two horizontal and two vertical wind power systems on the basis of energy and exergy. They analyzed each system on the basis of first two laws of thermodynamics. It was concluded that by using exergy methods, system can be made economical and more efficient as the exergy method clearly shows the amount of energy lost against irreversibilities. This enables the researcher to determine correct margin for improvement and targeted efforts can be made for efficiency improvement. In this way, it helps in increasing the capability of “wind energy system” through better site selection and efficient design of turbine [38]. The equations used for the energy efficiency ‘ $\eta$ ’ are given below:

$$\eta = \frac{\dot{W}_o}{E} \quad (4)$$

where

$$E = \text{Energy per unit time of the wind stream} = \frac{1}{2} \rho A V_\infty^3 \quad (5)$$

Similarly, the equations used for exergy efficiency ‘ $\psi$ ’ are as under;

$$\psi = \frac{\dot{W}_o}{Ex_f} \quad (6)$$

where

$$\text{Flow exergy} = Ex_p - Ex_K \quad (7)$$

$$Ex_p = \dot{m} \left[ C(T_2 - T_1) + T_o \left( C \ln \frac{T_2}{T_1} - R \ln \frac{P_2}{P_1} - \frac{C(T_o - T_{avg})}{T_o} \right) \right] \quad (8)$$

and

$$Ex_K = \frac{1}{2} \rho A V_\infty^3 - \frac{1}{2} \rho A V_2^3 \quad (9)$$

The values of ‘ $\dot{W}_o$ ’ are obtained by the product of torque (obtained through numerical prediction) and rotational velocity (obtained through simulation).

The results obtained by Pope et al. [38] indicated a difference of 44–55% between energy and exergy efficiency of VAWTs. This indicates a scope for further improvement in the current VAWT designs.

### 3.1.5. Computational fluid dynamics (CFD)

CFD has now become a powerful tool of fluid mechanics which analyzes and solves the problems related to fluid flows, utilizing numerical methods and algorithms with the help of electronic computers. Use of CFD can save time as well as expensive experimentation and is also being employed for improvement in vertical

axis wind turbine analysis. Well tuned CFD models can simulate the actual flow conditions which can produce results in close agreement with experimental outcomes. Hence design optimization can be done prior to entering the experimentation phase.

CFD analysis has been extensively used for the determination of coefficient of power for various wind turbine configurations. 2-D or 3-D models of wind turbine blade is created using CAD software and are meshed and solved with the help of computers to obtain the desired results.

The quantitative findings of CFD analysis for various VAWT configurations have been discussed in detail in the previous section. These findings, when compared, reveal that high values of  $C_p$  ( $\sim 0.38$ ) can be obtained for very low values of TSR ( $\sim 0.4$ ). When compared with HAWT, this can prove to be a big advantage. For Darrieus rotor, the  $C_p$  value increases up to an optimum value of TSR and then tends to decrease. For other configurations, i.e. Savonius, twisted three bladed rotor and H-rotor, same variation in  $C_p$  is observed with the increase in TSR. CFD results predicted by Howell et al. [18], Mohamed et al. [29] and Debnath et al. [30] are in good agreement to the experimental results for all the configurations. Hence CFD is well capable of predicting  $C_p$  for all the configurations.

### 3.2. Aerodynamic load calculations

The term ‘aerodynamic load’ refers to the forces acting and hence the stresses induced in the blades of a rotor as it rotates due to the wind flow around it. The calculation of these stresses is very important for the selection of blade material and blade cross section. Following are a few methods adopted by different researchers to carry out these calculations.

#### 3.2.1. Blade element method

The earliest and the most commonly used method for the calculation of aerodynamic loads on wind turbine blades is the blade element momentum method [39] developed by Gluert in 1963 and reviewed by Hansen et al. [39] for airfoil load calculations in aviation industry. This method is a combination of blade element theory and momentum theory. The calculations are performed by considering each element of the rotor as an independent entity. The calculations of thrust force on the blade and the torque are made using following equations:

$$C_{F_T} = \frac{dF_T}{1/2 \rho V_o^2 dA} \quad (10)$$

where ‘ $C_{F_T}$ ’ is a constant which can be calculated from the following equation:

$$C_{F_T} = 4dF \left( \frac{1}{f_g \cdot d} \right) \quad (11)$$

Once the thrust force ‘ $F_T$ ’ is known, the torque is obtained by multiplying it with the radius of the rotor which can then be used to calculate the stresses induced.

A comparison of results calculated from the formulas with the experimental values show a reasonable agreement between the two.

#### 3.2.2. Actuator disc method

Actuator disc theory was proposed by Gluert, as described by Islam et al. [23], to calculate the drag forces and hence aerodynamic loads on the blades. The equation used for the calculation is written here,

$$F_D = A \rho V_a (V_\infty - V_w) \quad (12)$$

where, ‘ $V_a$ ’ is the induced velocity; ‘ $V_\infty$ ’ is the free stream velocity and ‘ $V_w$ ’ is the wake velocity.

Actuator disc methods were also used by Madsen in 1982 for the determination of loads on wind turbines and were reviewed by Hansen et al. [39]. Madsen combined the Navier–Stokes (NS) equations with a non-steady structural model to simulate aero elastic response of wind turbine. This method is more accurate however computationally intensive than blade element momentum method. It considers all engineering adds-on such as dynamic wake, dynamic stall, and a yaw model to obtain realistic results. It also provides advantage of calculation of wake effect.

### 3.2.3. Dynamic analysis

Basic angular momentum equations of Engineering Mechanics, shown as under, were used by Biswas et al. [40] in 1995 to calculate the forces acting on the blades of a Darrieus rotor.

$$\left[ \frac{d\mathbf{H}_A}{dt} \right]_{XYZ} = \left[ \frac{d\mathbf{I}_\alpha}{dt} \right]_{xyz} + \mathbf{I}(\alpha) \left[ \frac{d\boldsymbol{\omega}}{dt} \right]_{xyz} + \boldsymbol{\Omega} \times [\mathbf{I}(\alpha)]\boldsymbol{\omega} \quad (13)$$

In the above equations, ' $\mathbf{H}_A$ ' represents angular momentum; ' $\mathbf{I}$ ' represents the inertia of the blade; ' $\boldsymbol{\omega}$ ' is the angular velocity and ' $\boldsymbol{\Omega}$ ' is the operational frequency; subscripts 'XYZ' being used for stationary axes and 'xyz' for rotating axes.

Eighteen equations were thus developed for the rotor, considering various degrees of freedom and were solved using computer codes developed in MS-DOS FORTRAN. Plots of stresses were generated against the ambient wind flow speeds using the equations solved at the two computer codes (VAWTDYN and AERODYNE). A reasonable agreement was observed between the calculated values and experimental data obtained previously by researchers at Sandia Laboratories [41].

### 3.2.4. Impulsive methods

Kopeika and Tereshchenko [36] described the impulsive method of load calculation in which the calculation relies on the relation between impulse loss of the flow going through the area swept by the rotor and the averaged-in-time of total aerodynamic force which is applied to the blades.

### 3.2.5. Vortex methods

Kopeika and Tereshchenko [36] also discussed the vortex models for load calculations on rotor blades. They have modeled non-stationary structure of streamlines for every rotor blade using vortex lattice method. No quantitative findings are however discussed by them in the paper.

Ponta and Jakovkis [42] described the equations involved in the calculation of stresses and other parameters of Darrieus wind turbine analysis with Vortex Model. The equations for stresses are simplified to the following form:

$$\tau = \frac{2K\rho U}{\delta} \quad (14)$$

In the above equation, ' $\tau$ ' is the stress induced in the rotor blade, ' $K$ ' is the kinematic viscosity, ' $\rho$ ' is the density of air, and ' $\delta$ ' is the boundary layer thickness.

Wilhelm et al. [26] developed 'Vortex Analytical Model' for aerodynamic load calculations. It measured vortices' circulation strength and location which was then used to estimate the velocity of air around the rotor at any point. The velocity measurements were then used to estimate the rotor performance under different flow conditions. The advantages of this model include its ability to determine blade-wake interactions, estimate results in unsteady flow conditions and for finite aspect ratios of rotor blades.

The vortex methods can also be used for the determination of aerodynamic coefficients and efficiency of the turbine.

## 3.3. Flow field visualization and analysis

Visualization of flow field around the wind turbine facilitates in understanding and analyzing the aerodynamic behavior of wind turbine. This ultimately helps in improving the design and efficiency of the device.

### 3.3.1. Particle image velocimetry

In 1998, Fujisawa and Takeuchi [43] used dye injection technique to visualize flow field in the region of a Darrieus rotor during dynamic stall. In this technique, a colored dye is bled into the flowing fluid and flow pattern is observed through the dye track [44]. They used particle image velocimetry (PIV) with a conditional imaging technique to measure phase averaged velocity distributions around the blade.

In PIV, tracer particles of specific weight nearly equal to the flowing fluid are injected in the fluid without affecting its velocity. These particles move with the same velocity as the local velocity of fluid. Pictures of moving particles at any instant of time in a flowing field are captured with the help of digital camera. Then these pictures are analyzed to get velocity of fluid at that instant [45].

They concluded that the phenomenon of dynamic stall appears due to shedding of two pairs of vortices from blade during one rotation of rotor. At low tip speed ratios ( $\lambda < 3$ ) of rotor, incidence angle varies and separation of flow field occurs, which produces dynamic stall of flow over rotating blade. The developed stall vortices interact with flow field near the blade and affect the aerodynamic performance of rotor. Moreover, dynamic stall is a prominent phenomenon at low tip speed ratios.

### 3.3.2. Computational fluid dynamics (CFD)

Flow field visualization through CFD can be found in the earlier works of Howell et al. [18] and Debnath et al. [30] CFD techniques have also been used for flow field visualization of a VAWT. In 2010, Wang et al. [46] used two URANS models that are standard  $k-\omega$  and shear stress transport  $k-\omega$  of CFD for simulation of dynamic stall phenomenon at low Reynolds number ( $Re_c \approx 10^5$ ). Relatively low computational cost and reasonable accuracy are attractive features of these models. After comparing the results of these models with experimental ones, they found that SST  $k-\omega$  model was better than the standard  $k-\omega$  model. SST  $k-\omega$  model efficiently captured the main features of dynamic stall phenomenon such as the aerodynamic load hysteresis and "LEV-dominated flow structure".

Large eddy models are more advanced and capable than URANS models. They require more computational time but provide better accuracy of results. Out of the two Large eddy (LE) models, DES and LES, DES model is better as the results estimated by it closely match with the experimental ones. DES model is combination of LES and URANS models. It is not only computationally cheaper than LES model but also models the wall region more accurately [47].

## 3.4. Vibration and fatigue calculation

With the passage of time, progress in wind turbines increased overall size of wind turbines resulting increase of vibrations. Hence, measurement of modal frequencies became utmost important in the design of wind turbines to avoid resonance and fatigue.

### 3.4.1. Operational modal analysis

Carne and James [48] reviewed the operational modal analysis techniques for wind turbines. Modal testing of wind turbines and blades started in late 1970s. Initially, Standard model testing technique was used which utilized artificial source of excitation such as step relaxation. It was very much time consuming because the apparatus was reloaded for every new input value, which meant



that turbine was brought to parked conditions first and then tested for new speed.

In 1986, the idea of utilizing natural wind for excitation of wind turbines or other large structures was presented. In 1988, this idea was utilized on 110 m tall wind turbine. As it was a new concept so step relaxation technique was also used along with NExT, an initial stage of OMA. Results obtained from NExT were closer to step relaxation technique which proved its success.

In 1993, a cross correlation function was developed which compared the output values without any need of input values. This cross correlation function could be directly used in the software for calculation of modal parameters.

To check the capability of NExT, results obtained from it were compared with analytically simulated data in 1996. For the purpose, a simulation code VAWT-SDS was developed and modal parameters were calculated. The results obtained from NExT were in good agreement with analytically simulated data.

OMA fails to predict model parameters properly in presence of harmonic excitations. In 2003, Mohanty and Rixen proposed a Single Station Time Domain (SSTD) method which accurately estimates Eigen frequencies and model parameters even when harmonic frequencies are closer to them [49].

Moreover, results obtained from NExT successfully verified conventional model test results. NExT has also been applied for measurement of modal frequencies and damping ratios for both HAWT and VAWT. NExT, which is now called as OMA, can determine both structural and aero-elastic, total system damping of an operating turbine [48].

### 3.5. Analysis of an attachment on blade

Attachments such as layer of snow, icing, and dust change both weight and profile of blades. So analysis of such an attachment is necessary for design purposes as it affects the overall performance of wind turbine.

#### 3.5.1. Wind tunnel testing

In 2010, Li et al. [50] designed a prototype of straight blade VAWT with three blades for wind tunnel test and studied the effects of attachment on blade. To make the analysis simple, they only simulated the condition of rime-type icing on leading edge of blade by employing clay instead of ice due to practical difficulties and measured the effects on power coefficient and rotation through wind tunnel tests.

It was concluded that the attachment reduces the rotation and power coefficient of wind turbine and these rates increase with wind speed and mass of attachment. Also, they believed that these changes were due to variations of aerodynamic characteristics of blade due to change of blade profile and uneven mass distribution due to attachment.

## 4. Conclusion

Vertical axis wind turbine offer economically viable energy solution for remote areas away from the integrated grid systems. In order to spread the use of VAWT, the problems associated with various configurations, i.e. poor self-starting and low initial torque, low coefficient of power, poor building integration should be overcome. Furthermore, following conclusions can be drawn from the present review:

1. Ample wind energy potential is available in the world. In order to make best use of it efficient designs of wind turbines need to be developed.

2. Various vertical axis wind turbines can offer solution to the energy requirements ranging from 2 kW to 4 MW with a reasonable payback period.
3. Coefficient of power can be maximized by selecting a suitable TSR range for various configurations.
4. VAWTs offer good possibility of building integrated designs. Crossflex type VAWT can be used on high rise buildings in the cities where free stream velocity greater than 14 m/s is available. Similarly, Sistan type wind turbine can be effectively integrated with building designs and can give reasonable power output.
5. CFD is capable of designing the VAWT with higher degree of accuracy. It can also be used for the optimization of blade design. Moreover, flow field around various configurations' blades can also be visualized with the help of CFD. It has not only accelerated the design process of VAWT but also has brought down the overall cost of designing.
6. Calculation of Exergy efficiency can give a better understanding of the losses occurring in the VAWTs due to irreversibilities. Targeted efforts can then be made to overcome these losses.

## References

- [1] Baker JR. Features to aid or enable self starting of fixed pitch low solidity vertical axis wind turbines. *Journal of Wind Engineering and Industrial Aerodynamics* 2003;15:369–80.
- [2] Ponta FL, Seminara JJ, Otero AD. On the aerodynamics of variable-geometry oval-trajectory Darrieus wind turbines. *Renewable Energy* 2007;32:35–56.
- [3] Chaichana T, Chaitap S. Wind power potential and characteristic analysis of Chiang Mai, Thailand. *Mechanical Science and Technology* 2010;24:1475–9.
- [4] Loth JL. Aerodynamic tower shake force analysis for VAWT. *Journal of Solar Energy Engineering* 1985;107:45–50.
- [5] Homicz GF. VAWT stochastic loads produced by atmospheric turbulence. *Journal of Solar Energy Engineering* 1989;111:358–67.
- [6] Bishop JKD, Amaratunga GAJ. Evaluation of small wind turbines in distributed arrangement as sustainable wind energy option for Barbados. *Energy Conversion and Management* 2008;49:1652–61.
- [7] Islam M, Fartaj A, Ting DSK. Current utilization and future prospects of emerging renewable energy applications in Canada. *Renewable and Sustainable Energy Reviews* 2004;8:493–519.
- [8] Gorelov DN. Analogy between a flapping wing and a wind turbine with a vertical axis of revolution. *Applied Mechanics and Technical Physics* 2009;50:297–9.
- [9] Gorelov DN, Krivospitsky VP. Prospects for development of wind turbines with orthogonal rotor. *Thermophysics and Aeromechanics* 2008;15:153–7.
- [10] Islam M, Ting DSK, Fartaj A. Aerodynamic models for Darrieus-type straight-bladed vertical axis wind turbines. *Renewable and Sustainable Energy Reviews* 2008;12:1087–109.
- [11] Eriksson S, Bernhoff H, Leijon M. Evaluation of different turbine concepts for wind power. *Renewable and Sustainable Energy Reviews* 2008;12:1419–34.
- [12] Marini M, Massardo A, Satta A. Performance of vertical axis wind turbines with different shapes. *Journal of Wind Engineering and Industrial Aerodynamics* 1992;39:83–93.
- [13] Shienbein LA, Malcolm DJ. Design performance and economics of 50-kW and 500-kW vertical axis wind turbines. *Journal of Solar Energy Engineering* 1983;105:418–25.
- [14] Brahami MT, Paraschivoiu I. Darrieus rotor aerodynamics in turbulent flow. *Journal of Solar Energy Engineering* 1995;117:128–37.
- [15] Rosen A, Abramovich H. Investigation of the structural behavior of the blades of a Darrieus wind turbine. *Journal of Sound and Vibration* 1985;100:493–509.
- [16] Bergeles G, Michos A, Athanassiadis N. Velocity vector and turbulence in the symmetry plane of a Darrieus wind generator. *Journal of Wind Engineering and Industrial Aerodynamics* 1991;37:87–101.
- [17] Wakui T, Tanzawa Y, Hashizume T, Outa E, Usui A. Optimum method of operating the wind turbine-generator systems matching the wind condition and wind turbine type. *World Renewable Energy Congress* 2000;VI:2348–51.
- [18] Howell R, Qin N, Edwards J, Durrani N. Wind tunnel and numerical study of a small vertical axis wind turbine. *Renewable Energy* 2010;35:412–22.
- [19] Mertens S, van Kuik G, van Bussel G. Performance of an H-Darrieus in the skewed flow on a roof. *Journal of Solar Energy Engineering* 2003;125:433–41.
- [20] Staelens Y, Saeed F, Paraschivoiu I. A straight-bladed variable-pitch VAWT concept for improved power generation; 2003. p. 146–54.
- [21] Siota T, Isaka T, Sano T, Seki K. Matching between straight-wing nonarticulated vertical axis wind turbine and a new wind turbine generator. *Electrical Engineering in Japan* 2011;174:26–35.
- [22] Vandenberghe D, Dick E. A free vortex simulation method for the straight bladed vertical axis wind turbine. *Journal of Wind Engineering and Industrial Aerodynamics* 1987;26:307–24.
- [23] Islam M, Amin MR, Ting DSK, Fartaj A. Aerodynamic factors affecting performance of straight-bladed vertical axis wind turbines. In: *ASME international mechanical engineering congress and exposition*, vol. 6. 2007. p. 331–41.



- [24] Graham IV HZ, Panther C, Hubbell M, Wilhelm JP, Angle II GM, Smith JE. Airfoil selection for a straight bladed circulation controlled vertical axis wind turbine. In: ASME 2009 3rd international conference on energy sustainability, vol. 1. 2009. p. 579–84.
- [25] Takao M, Kuma H, Maeda T, Kamada Y, Oki M, Minoda A. A straight-bladed vertical axis wind turbine with a directed guide vane row effect of guide vane geometry on the performance. *Journal of Thermal Science* 2009;18: 54–7.
- [26] Wilhelm JP, Panther C, Pertl FA, Smith JE. Momentum analytical model of a circulation controlled vertical axis wind turbine. In: ASME 3rd international conference on energy sustainability, vol. 2. 2009. p. 1009–17.
- [27] Gupta R, Biswas A. Computational fluid dynamics analysis of a twisted three-bladed H-Darrieus rotor. *Renewable and Sustainable Energy* 2010;2:1–15.
- [28] Sharpe T, Proven G. Crossflex: concept and early development of a true building integrated wind turbine. *Energy and Buildings* 2010;42:2365–75.
- [29] Mohamed MH, Janiga G, Pap E, Thévenin D. Optimal blade shape of a modified Savonius turbine using an obstacle shielding the returning blade. *Energy Conversion and Management* 2011;52:236–42.
- [30] Debnath BK, Biswas A, Gupta R. Computational fluid dynamics analysis of a combined three-bucket Savonius and three-bladed Darrieus rotor at various overlap. *Journal of Renewable and Sustainable Energy* 2009;1:1–13.
- [31] Gavalda J, Massons J, Diaz F. *Solar Wind Technology* 1990;7:457.
- [32] Zhang Q, Chen H, Wang B. Modelling and simulation of two leaf semi-rotary VAWT. *Zhongyuan Institute of Technology*; 2010. p. 389–398.
- [33] Al-Hassan AY, Hill DR. *Islamic technology: an illustrated history*. Cambridge Press, Cambridge University; 1986.
- [34] Muller G, Mark F, Jentsch MF, Stoddart E. Vertical axis resistance type wind turbines for use in buildings. *Renewable Energy* 2009;34:1407–12.
- [35] Pope K, Rodrigues V, Doyle R, Tsopelas A, Gravelsins R, Naterer GF, et al. Effects of stator vanes on power coefficients of a zephyr vertical axis wind turbine. *Renewable Energy* 2010;35:1043–51.
- [36] Kopeika OV, Tereshchenko AV. Wind power transforming systems. *Journal of Mathematical Sciences* 2001;104:1631–4.
- [37] Pope K, Naterer GF, Dincer I, Tsang E. Power correlation for vertical axis wind turbines with varying geometries. *International Journal of Energy Research* 2010;1703.
- [38] Pope K, Dincer I, Naterer GF. Energy and exergy efficiency comparison of horizontal and vertical axis wind turbines. *Renewable Energy* 2010;35:2102–13.
- [39] Hansen MOL, Sørensen JN, Voutsinas S, Sørensen N, Madsen HAa. State of the art in wind turbine aerodynamics and aeroelasticity. *Progress in Aerospace Sciences* 2006;42:285–330.
- [40] Biswas S, Sreedbhardt BN, Singh YP. Dynamic analysis of a vertical axis wind turbine using a new wind load estimation technique. *Computers and Structures* 1997;65:903–16.
- [41] Proceedings of the vertical axis wind turbine technology workshop, Albuquerque, Sandia Laboratories Report. SAND 76-5586. NM 17-20; 1976.
- [42] Ponta FL, Jacoviks PM. A vortex model for Darrieus turbine using finite element techniques. *Renewable Energy* 2001;24:1–18.
- [43] Fujisawa N, Takeuchi M. Flow visualization and PIV measurement of flow field around s Darrieus rotor in dynamic stall visualization. *Journal of Visualization* 1999;1:379–86.
- [44] Beckwith TG, Marangoni RD, Leinhard V JH. *Mechanical measurements*. sixth ed. India: Pearson Education; 2007.
- [45] Chung SK, Kim SK. Digital particle image velocimetry studies of nasal airflow. *Respiratory Physiology and Neurobiology* 2008;163:111–20.
- [46] Wang S, Ingham DB, Ma L, Pourkashanian M, Tao Z. Numerical investigations on dynamic stall of low Reynolds number flow around oscillating airfoils. *Computers and Fluids* 2010;39:1529–41.
- [47] Ferreira CS, Kuik GV, Busse GV, Scarano F. Visualization by PIV of dynamic stall on a vertical axis wind turbine. *Experiments in Fluids* 2009;46:97–108.
- [48] Carne TG, James GH. The inception of OMA in the development of modal testing technology for wind turbines. *Mechanical Systems and Signal Processing* 2010;24:1213–26.
- [49] Mohanty P, Rixen DJ. Modified SST method to account for harmonic excitations during operational modal analysis. *Mechanism and Machine Theory* 2004;39:1247–55.
- [50] Li Y, Tagawa K, Liu W. Performance effects of attachment on blade on a straight-bladed vertical axis wind turbine. *Current Applied Physics* 2010;10:S335–8.
- [51] SRC – Vertical. <http://www.eng.src-vertical.com/information/infbasic> [accessed 04.03.11].
- [52] Energy Efficient Choices. <http://www.energyefficientchoices.com/wind-turbine-power-energy/vertical-axis-wind-turbines.php> [accessed 04.03.11].



本文献由“学霸图书馆-文献云下载”收集自网络，仅供学习交流使用。

学霸图书馆（[www.xuebalib.com](http://www.xuebalib.com)）是一个“整合众多图书馆数据库资源，提供一站式文献检索和下载服务”的24小时在线不限IP图书馆。

图书馆致力于便利、促进学习与科研，提供最强文献下载服务。

#### 图书馆导航：

[图书馆首页](#)    [文献云下载](#)    [图书馆入口](#)    [外文数据库大全](#)    [疑难文献辅助工具](#)